Available online at www.sciencedirect.com
SCIENCE DIRECT®
Respiratory Physiology & Neurobiology 153 (2006) 66–77
RESPIRATORY PHYSIOLOGY & NEUROBIOLOGY
www.elsevier.com/locate/resphysiol

Deep diving mammals: Dive behavior and circulatory adjustments contribute to bends avoidance

A. Fahlman [a,*], A. Olszowka [b], Brian Bostrom [a], David R. Jones [a]

[a] *Department of Zoology, The University of British Columbia, 6270 University Blvd., Vancouver, BC, Canada V6T 1Z4*
[b] *Department of Physiology and Biophysics, The University at Buffalo, Buffalo, NY 14144, USA*

Accepted 6 September 2005

Abstract

A mathematical model was created that predicted blood and tissue N_2 tension (P_{N_2}) during breath-hold diving. Measured muscle P_{N_2} from the bottlenose dolphin after diving repeatedly to 100 m (*Tursiops truncatus* [Ridgway and Howard, 1979, Science, 4423, 1182–1183]) was compared with predictions from the model. Lung collapse was modelled as a 100% pulmonary shunt which yielded tissue P_{N_2} similar to those reported for the dolphin. On the other hand, predicted muscle P_{N_2} for an animal with a dive response, reducing cardiac output by 66% from surface values (20.5 to 6.8 $l \cdot min^{-1}$), also agreed well with observed values in the absence of lung collapse. In fact, modelling indicated that both cardiovascular adjustments and dive behaviour are important in reducing N_2 uptake during diving and enhancing safe transfer of tissue and blood N_2 back to the lung immediately before coming to the surface. In particular, diving bradycardia during the descent and bottom phase together with a reduced ascent rate and increase in heart rate reduced mixed venous P_{N_2} upon return to the surface by as much as 45%. This has important implications as small reductions in inert gas load (∼5%) can substantially reduce decompression sickness (DCS) risk by as much as 50% (Fahlman et al., 2001, J. Appl. Physiol. 91, 2720–2729).
© 2005 Elsevier B.V. All rights reserved.

Keywords: Decompression sickness; Modelling; Inert gas flux; Pressure; Decompression stop; Allometry

1. Introduction

During exposure to elevated environmental pressure increased amounts of inert gas dissolve in the tissues of air-breathing animals. The amount of inert gas dissolved is a function of the pressure and the duration of exposure. The tissue tension of dissolved inert gas continues to increase until equilibration occurs, at which time the organism is said to be saturated. If the decompression phase is too rapid, elevated levels of N_2 in blood or tissues exceed their solubility at the reduced pressure, a term called supersaturation. When N_2 becomes supersaturated in tissues, it comes out of solution possibly forming bubbles. In fact, detectable bubbles have been found in half the human subjects

* Corresponding author. Tel.: +1 604 822 5043; fax: +1 604 822 8121.
E-mail addresses: andreas_fahlman@yahoo.com, fahlman@zoology.ubc.ca (A. Fahlman).

1569-9048/$ – see front matter © 2005 Elsevier B.V. All rights reserved.
doi:10.1016/j.resp.2005.09.014

after decompression following a saturation dive to 3 m (1.3 ATA; Eckenhoff et al., 1990). At this time the tissue and blood N_2 tensions (P_{N_2}) should be ~1 ATA. Bubbles can block blood vessels and damage tissue, producing the medical condition called decompression sickness (DCS) or the bends. Some level of supersaturation and bubble formation may be tolerated, but current research suggests that any hyperbaric exposure has a finite probability of DCS (Weathersby et al., 1984, 1992).

The time it takes for a tissue to reach saturation, or equilibrium, after a change in pressure is dependent on the blood flow through that tissue (Hlastala and van Liew, 1975). This makes it possible to separate tissues into rapidly (e.g. heart) or slowly (e.g. fat) saturating tissues. Consequently, diving related vasoconstriction and bradycardia increases time to saturation and reduces the likelihood of reaching a tissue P_{N_2} that will cause bubble formation during decompression. Still, current estimates indicate that blood and tissue P_{N_2} in seals can be as high as 2–3 ATA during a single hyperbaric exposure without causing bends on decompression (Kooyman et al., 1972; Falke et al., 1985). Thus, in animals that dive repeatedly, elevated P_{N_2} levels could predominate for most of their lives. These P_{N_2} levels can cause severe DCS incidence in a significant proportion of non-diving mammals (Dromsky et al., 2000). Early research suggested that decompression was safe unless the rate of decrease in ambient pressure (P_{amb}) exceeded a certain critical value (Hills, 1977) but, it now seems that the occurrence of DCS is somewhat arbitrary, seldom either a certainty or zero for decompression from any given hyperbaric exposure (Weathersby et al., 1992). In addition, the probability of DCS increases with body mass (M_b, Berghage et al., 1979; Lillo et al., 1985, 1997, 2002; Lillo, 1988). Therefore, one "safe" tissue P_{N_2} ($P_{N_{2_{tiss}}}$) cannot be assumed to apply to all breath-hold diving animals.

While repetitive breath-hold dives to 15–20 m have been reported to cause DCS in humans (Paulev, 1965, 1967), seals or dolphins are not reported to develop the bends during continuous diving. This suggests either adaptations that deal with an elevated bubble load or an ability to avoid supersaturation. An adapted immune system, which is less reactive to bubbles, could prove to be important since a connection between immune function and DCS has been shown (Ward et al., 1987; Kayar et al., 1997). Lung collapse has been suggested as a universal mechanism that reduces supersaturation and therefore, the risk of DCS in breath-hold diving mammals. Indirect measurements suggest that in seals and dolphins alveolar collapse occurs at approximately 40–80 m, reducing the amount of N_2 available to equilibrate with the tissues (Ridgway and Howard, 1979; Falke et al., 1985). Weddell and elephant seals are reported to dive upon exhalation further reducing the available N_2.

Thus, a better understanding of the inert gas flux of diving animals would enhance our understanding how they can perform repeated dives without developing $P_{N_{2_{tiss}}}$ levels that may be harmful. Therefore, we created a mathematical model to describe P_{N_2} in blood and tissues during repeated breath-hold dives. The model was a simplified version of that used to trace metabolic and inert gases in human breath-hold divers (Olszowka and Rahn, 1987). However, our model accounts for changes in blood perfusion and also incorporates the possibility of a pulmonary shunt where blood bypasses the blood–gas exchange surface. We validated model predictions against data for the bottlenose dolphin (Ridgway and Howard, 1979), as this is the only animal in which both dive sequence and muscle P_{N_2} have been reported for voluntary repeated breath-hold diving.

2. Materials and methods

2.1. Model

The model was adapted from the human breath-hold model developed by Olszowka and Rahn (1987) and is outlined in Fig. 1. The body was partitioned into five different compartments or stores; blood, brain, fat, muscle and a central circulatory compartment. The central circulatory compartment included heart, kidney, liver and alimentary tract while the fat compartment included fat, skin, bone and connective tissue.

Gas exchange occurred between lung and blood and between blood and each compartment (Fig. 1A–D). The N_2 store in the lung consisted only of a gas phase and was assumed to be perfectly mixed. We assumed that there was no diffusion resistance at the lung surface (Farhi, 1967). All pressures were corrected for water vapor pressure, assuming that the respiratory system was fully saturated at 37 °C. We

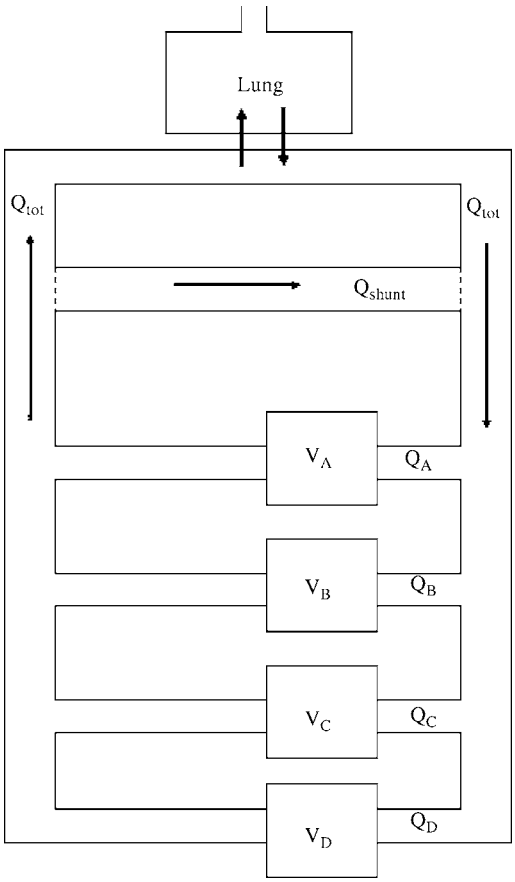

Fig. 1. An outline of the model showing gas exchange between blood and lung. Total blood flow ($\dot{Q}_{tot}$) was divided into tissue specific flows ($\dot{Q}_A - \dot{Q}_D$) in each of the four compartments. V_A–V_D denote the volumes of the four compartments.

used an inspired fraction of N_2 (F_{N_2}) of 79% before a breath-hold and for the first breath-hold it was assumed that the animal was in a steady state and $P_{N_{2_{tiss}}}$ was 0.74 ATA, i.e. full saturation. We assumed that F_{N_2} was 79% at all times both at the surface and while diving. Thus, alveolar N_2 partial pressure (Pa_{N_2}) was equal to the product between P_{amb} and F_{N_2}. Furthermore, arterial blood tension of N_2 (P_{N_2blood}) was assumed equal to Pa_{N_2}. Alveolar collapse was assumed to occur instantaneously at a pre-determined depth (Ridgway and Howard, 1979; Houser et al., 2001). We assumed that N_2 was depleted once total lung N_2 (number of molecules) had decreased to <1% of the initial amount. During alveolar collapse, i.e. 100% pulmonary shunt, or once lung N_2 was depleted, exchange with the lung stopped until flux of N_2 was reversed. During ascent we assumed that the lung was re-inflated at the same depth at which collapse occurred during descent.

Blood N_2 stores were broken down into arterial and venous compartments being 1/3 and 2/3 of the total blood volume, respectively. Total blood volume was divided into smaller variable volumes (blood packages) equal to the product of the cardiac output ($\dot{Q}_{tot}$, $l \cdot s^{-1}$) and the time step (Δt, s) used in the numerical integration of the mass balance equation (Olszowka and Rahn, 1987). Blood packages are transported around the circulatory system as if being on a conveyer belt. During each time step, one mixed venous package was accessible for gas exchange at the lung and an arterial package was accessible to the tissue compartments. The remaining packages accounted for the transit time. Before gas exchange at each tissue compartment, the arterial package was divided into four smaller volumes, representing blood flow to each compartment ($\dot{Q}_{tiss}$). The estimated metabolic rate of a tissue ($\dot{V}_{O_2 n}$) divided by the total metabolic rate ($\sum_{n=1}^{4} \dot{V}_{O_2 n}$) was used to partition the arterial package into the smaller volumes. $\dot{Q}_{tot}$ or the fraction of blood to each tissue were not fixed and could be varied to mimic diving bradycardia and changes in regional blood flow due to peripheral vasoconstriction. Hence, cardiovascular changes seen in freely diving animals could be simulated (Zapol et al., 1989; Andrews et al., 1997; Froget et al., 2004). After tissue gas exchange, the four smaller blood volumes joined to re-form a package.

The Ostwald solubility coefficient of N_2 for blood was taken to be 0.0144 ml $N_2 \cdot$ml blood^{-1} (Weathersby and Homer, 1980). The N_2 solubility in fat was given a tissue–blood partition coefficient of five while for all other tissues it was assumed that N_2 solubility was identical to that of blood (Weathersby and Homer, 1980).

The dolphin data reported by Ridgway and Howard (1979) was used to validate our model. In the instances where we had no direct anatomical or physiological data for the dolphin, we used data reported for the Weddell seal (Davis and Kanatous, 1999), assuming that there were no differences between the bottlenose dolphin and the Weddell seal except for M_b. Thus, the relative size of each compartment remained constant (fat: 36%, muscle: 38%, central circulatory: 4%, brain: 0.5%, blood: 21.5%). Resting metabolic rate (897 ml $O_2 \cdot min^{-1}$) and resting cardiac output (42.7 $l \cdot min^{-1}$) were adjusted for differences in M_b

using a scaling mass-exponent of 0.75. The lung (LV) and blood (BV) volumes for bottlenose dolphin (LV = 81 ml·kg^{-1}, BV = 71 ml·kg^{-1}) were taken from Kooyman and Ponganis (1998). Lung volume was scaled as a constant fraction of M_b (Schmidt-Nielsen, 1984) which is the case for a wide range of mammals. The mass-adjusted metabolic rate of each compartment for the Weddell seal (CS) was assumed to scale to M_b with a mass exponent of 0.75. Thus, the equation used to estimate organ mass-specific $\dot{V}_{O_2}$ for each compartment (C) was:

$$(\dot{V}_{O_2})_C = (\dot{V}_{O_2})_{CS} \cdot \frac{(M_b^{-0.25})_C}{(M_b^{-0.25})_{CS}} \quad (1)$$

For the central circulatory compartment, the mass-adjusted $\dot{V}_{O_2}$ for heart, liver and kidney was computed and summed. Blood flow to each compartment was assumed to be directly proportional to $\dot{V}_{O_2}$ for that compartment relative to total $\dot{V}_{O_2}$ (see above).

2.2. Computations

Mass balance equations were used to follow gas transport in the lungs and tissues over a short time interval (Δt) and small blood volumes (package volume), using P_{N_2} as the driving force for gas exchange. To save computational time, the temporal resolution, i.e. Δt, was set to 1 s as no significant differences in output of the model was found at $\Delta t < 1$ s. For the blood volume in contact with each compartment or the lung, mass balance was expressed as an equality between the change in the amount of N_2 in the blood and the amount of gas removed from or added to each compartment during Δt. For exchange between lung and blood, the transfer of gas was calculated over each Δt, accounting for changes in P_{amb}.

An exponential gas kinetics model was used to estimate tissue and blood P_{N_2} (Kety, 1951; Fahlman et al., 2001). In other words, each compartment was considered to be composed of a single homogenous tissue, with a single perfusion rate and tissue gas solubility (S_{tiss}). The following differential equation was used to describe the inert gas tissue tension:

$$\frac{dP_{N_2tiss}}{dt} = \frac{(P_{N_2blood} - P_{N_2tiss}) \cdot \dot{Q}_{tiss}}{V_{tiss}} \cdot \frac{S_{blood}}{S_{tiss}} \quad (2)$$

where V_{tiss} is the tissue volume (L) and S_{blood} is the solubility of N_2 in blood. Assuming that perfusion rate is constant over Δt, several terms can be expressed as a single tissue specific time constant (τ_{tiss});

$$\tau_{tiss} = \frac{V_{tiss}}{\dot{Q}_{tiss}} \cdot \frac{S_{tiss}}{S_{blood}} \quad (3)$$

and

$$\frac{dP_{N_2tiss}}{dt} = \frac{(P_{N_2blood} - P_{N_2tiss})}{\tau_{tiss}} \quad (4)$$

2.3. Model parameters

To test the effect of changes in $\dot{Q}_{tot}$, $\dot{Q}_{tiss}$, and perfusion distribution separately, we created a hypothetical saturation dive. This hypothetical situation was not intended to reflect a real-life situation, but simplified the estimation of τ values.

The hypothetical saturation dive consisted of an instantaneous compression to 24 ATA (i.e. 24 ATA·s^{-1}) where the animal remained until all tissues were saturated. We assumed a marine mammal with M_b = 100 kg, $\dot{Q}_{tot}$ = 13.8 l·min^{-1} in which 67, 13, 18, and 2% of $\dot{Q}_{tot}$ were directed to the central circulatory, fat, muscle and brain, respectively both at the surface and during diving. Computed τ values were used to calculate time to 50% completion ($\tau_{1/2}$) of inert gas uptake as $\tau_{1/2} = \ln 2 \times \tau$ (Fahlman and Kayar, 2003), where ln is the natural logarithm. The time required to reach a certain fractional transformation to the new saturated steady state, say 95 or 99%, was computed as $3 \times \tau$ and $4.6 \times \tau$, respectively (Fahlman and Kayar, 2003). The resulting $\tau_{1/2}$ for this hypothetical saturation dive was therefore, 0.3 min for central circulation, 68.6 min for fat, 9.7 min for muscle and 6.7 min for brain.

We also wanted to determine the time course of N_2 depletion in the lung. During a breath-hold dive the lung contains a finite amount of N_2 that will diffuse into the blood and tissues. Depletion of N_2 was assumed to be when <1% of the initial number of molecules remained in the lung. Three dive profiles to pressures of 4, 14 and 24 ATA were used, all with a compression rate of 0.1 ATA·s^{-1}. The animal remained at depth until the lung N_2 was depleted (max 60 min). This dive duration was necessary to estimate the time for total lung N_2 depletion. Two different body masses were used (100 and 1000 kg) and the fraction of blood package volume flowing to each compartment was in proportion to their metabolic rate as described above.

2.4. Application of the model to dolphin data

We used the data from two dolphins presented by Ridgway and Howard (1979) performing dive bouts consisting of repeated voluntary dives (23 and 25 dives, respectively) to 100 m. After the last dive in the series, muscle P_{N_2} was recorded in both animals every 30 s from 8 until 22 min. Muscle P_{N_2} values were estimated from Fig. 2 in Ridgway and Howard (1979) for each of the two animals and converted to ATA. Body masses of these animals were 130 and 133 kg (Ridgway, Pers. Comm.).

For the simulations, we assumed a single animal with a M_b of 130 kg. The simulations assumed a series of 24 repeated dives to 100 m. This dive bout lasted for 1 h and each dive had a total dive time (DT) of 90 s (including ascent and descent). Each dive was interspersed by a 60 s surface interval (SI). We assumed a constant and symmetrical descent and ascent rate of 2.2 m·s^{-1}. From the dolphin data, the average muscle $\tau_{1/2}$ for N_2 removal was estimated to be 5.9 min (Ridgway et al., 1979). We therefore, adjusted $\dot{Q}_{tot}$ to 20.5 l·min^{-1} instead of the resting value of 16.8 l·min^{-1} estimated from allometric scaling. In addition, the fraction of $\dot{Q}_{tot}$ directed to the muscle compartment was increased to 27% and fat decreased to 4%. This dive series, or dive bout, was our base model (series A, Table 1) against which we compared changes in blood and tissue P_{N_2} with changes in behavioral and physiological variables.

To test the effect of changes in pulmonary shunt (0–90% of total pulmonary blood flow), ascent/descent rate (2.2–5.0 m·s^{-1}), SI (20–240 s) and DT (90–240 s) and cardiovascular adjustment (dive response) on mixed venous and muscle P_{N_2}, dive series A was used and one variable at a time was altered (Table 1). One dive series (series P, Table 1) simulated a staged decompression, where ascent rate decreased upon approaching the surface. Thus, series P was identical to series A, until the animal reached a depth of 30 m when the rate of ascent decreased to 1 m·s^{-1}. At 5 m of depth, rate of ascent again decreased to 0.5 m·s^{-1} until the animal reached the surface (Table 1). Dive series F and Q are similar to series A and P, respectively but include a dive response where $\dot{Q}_{tot}$ during diving was set to 1/3 of the surface value. To simulate pre-surface increase in heart rate, the animal in series Q experienced a reversal of the diving bradycardia at 30 m below the surface during ascent.

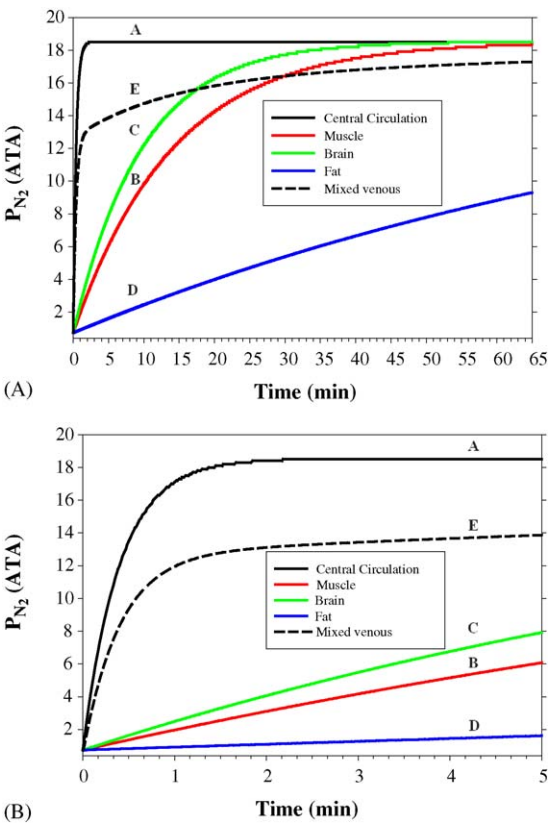

Fig. 2. The estimated central circulatory (A), muscle (B), brain (C), fat (D) and venous compartment P_{N_2} (E) during a hypothetical saturation dive to 24 ATA for a 100 kg dolphin. $\dot{Q}_{tot}$ was 13.8 l·min^{-1} and the perfusion distribution 67, 18, 2 and 13% to the central circulatory, muscle, brain and fat compartments, respectively with no shunt. Panel A shows the tissue and venous P_{N_2} for the first 65 min at depth and panel B the same data for the first 5 min.

3. Results

3.1. Model characteristics

A change in $\dot{Q}_{tot}$ directly affected $\tau_{1/2}$ of the whole animal. Hence, a 50% decrease in $\dot{Q}_{tot}$ without a change in blood flow distribution increased $\tau_{1/2}$ by a factor of two. Similarly, a change in $\dot{Q}_{tiss}$ affected $\tau_{1/2}$ for that compartment and also $\tau_{1/2}$ of the whole animal. Simultaneous changes in $\dot{Q}_{tot}$ and blood flow distribution to the various compartments, affected both $\tau_{1/2}$ of the

Table 1
Dive series, dive time (DT, s), surface interval (SI, s), dive time and surface interval ration (DT/SI), descent (D, m·s^{-1}) and ascent rates (A, m·s^{-1}) for a 130 kg bottlenose dolphin during a dive bout with 24 dives to a depth of 100 m

Dive series	DT	SI	DT/SI	D	A	Shunt fraction	Muscle P_{N_2}	Mixed venous P_{N_2}
A	90	60	1.5	2.2	2.2	0	3.15	4.02
B	90	60	1.5	2.2	2.2	30	2.77	3.64
C	90	60	1.5	2.2	2.2	50	2.40	3.18
D	90	60	1.5	2.2	2.2	70	1.90	2.47
E	90	60	1.5	2.2	2.2	90	1.20	1.44
F	90	60	1.5	2.2	2.2	0	2.03	3.21
G	90	60	1.5	3.0	2.2	0	3.47	4.23
H	90	60	1.5	5.0	2.2	0	3.86	4.45
I	90	60	1.5	2.2	3.0	0	3.52	4.68
J	90	60	1.5	2.2	5.0	0	3.88	5.70
K	180	60	3	2.2	2.2	0	5.22	5.02
L	240	60	4	2.2	2.2	0	5.92	5.25
M	90	20	4.5	2.2	2.2	0	3.90	4.25
N	90	90	1	2.2	2.2	0	2.80	3.92
O	90	240	0.375	2.2	2.2	0	2.03	3.69
P	90	60	1.5	3.0	2.2	0	2.94	2.72
Q	90	60	1.5	3.0	2.2	0	1.98	2.20

Dive series, shunt fraction (0–90%, Fig. 4), venous and muscle P_{N_2} (ATA) upon surfacing from the last dive in the dive series. For dive series P and Q the ascent rate was stepped being 2.2 m·s^{-1} until a depth of 30 m, then 1.0 m·s^{-1} until a depth of 5.0 m and then 0.5 m·s^{-1} until reaching the surface. Dive series F and Q included a dive response. For dive series Q, the diving bradycardia was reversed during the ascent at a depth of 30 m.

whole animal as well as each compartment. A higher flow to compartments with a larger N_2 capacitance, i.e. larger V_{tiss} or higher S_{tiss}, without a change in $\dot{Q}_{tot}$ increased $\tau_{1/2}$ of the whole animal. Thus, time to saturation of the whole animal was dependent on $\dot{Q}_{tot}$ as well as blood flow distribution.

Changes in tissue and mixed venous P_{N_2} during a saturation dive to 24 ATA for a 130 kg dolphin is shown in Fig. 2. Mixed venous P_{N_2} was a complex composite of the four compartments. Initially, mixed venous P_{N_2} was governed by the highly perfused and rapidly saturating central circulatory compartment P_{N_2} (Fig. 2A). As central circulatory P_{N_2} asymptotically approached saturation at ∼72 s, mixed venous P_{N_2} rapidly increased from 0.74 to ∼13 ATA (Fig. 2B). Next, mixed venous P_{N_2} slowly increased as muscle and brain tissues approached saturation. Once the central circulatory, muscle and brain compartments were saturated, after 50–65 min (Fig. 2A), mixed venous P_{N_2} was governed by P_{N_2} increases in the fat compartment.

Without a diving bradycardia (LV = 81 ml·kg^{-1}, 1000 kg, $\dot{Q}_{tot}$ = 77.8 l·min^{-1}; 100 kg, $\dot{Q}_{tot}$ = 13.8 l·min^{-1}) or pulmonary shunt, lung N_2 in a 1000 kg mammal was depleted after ∼190, ∼100 and ∼100 s for compressions to 4, 14 and 24 ATA, respectively. N_2 depletion in a 100 kg mammal were >60 min, 580 and 345 s.

3.2. Application of the model to dolphin data

In Fig. 3, the solid line A is estimated muscle P_{N_2} without lung collapse. This resulted in a maximum muscle P_{N_2} of 3.15 ATA at the end of the dive bout. The solid line B shows the same dive series, but assuming an instantaneous lung collapse, i.e. 100% pulmonary shunt, at 70 m. For both the lines A and B it is assumed that $\dot{Q}_{tot}$ and $\dot{Q}_{muscle}$ were 20.5 and 5.5 l·min^{-1}, respectively while diving and during the surface interval, representing symmetrical muscle N_2 uptake and removal rate, i.e. $\tau_{1/2}$ = 5.9 min The solid lines D and C are estimated muscle P_{N_2} for an animal with and without lung collapse, combined with a dive response. In this case, $\dot{Q}_{tot}$ during diving was 33% (6.8 l·min^{-1}) of that during the surface interval (20.5 l·min^{-1}) and muscle $\tau_{1/2}$ was 5.9 min at the surface and 17.5 min during diving. The black brackets encompass the ranges of expected muscle P_{N_2} with or without lung collapse at 70 m as calculated by Ridgway and Howard (1979). Filled and open symbols are observed muscle P_{N_2} from two dolphins at 8

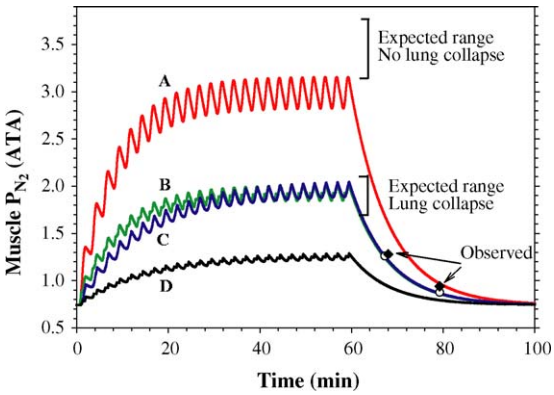

Fig. 3. Increase during diving and decrease after surfacing in muscle P_{N_2} for a 130 kg bottlenose dolphin performing 24 repeated dives to 100 m with a dive time of 1.5 min, a surface interval of 1 min and an ascent/descent rate of 2.2 m·s^{-1}. Black brackets shows estimated range of muscle P_{N_2} with and without lung collapse. Open and closed symbols indicate observed values for two animals (Ridgway and Howard, 1979; Houser et al., 2001).

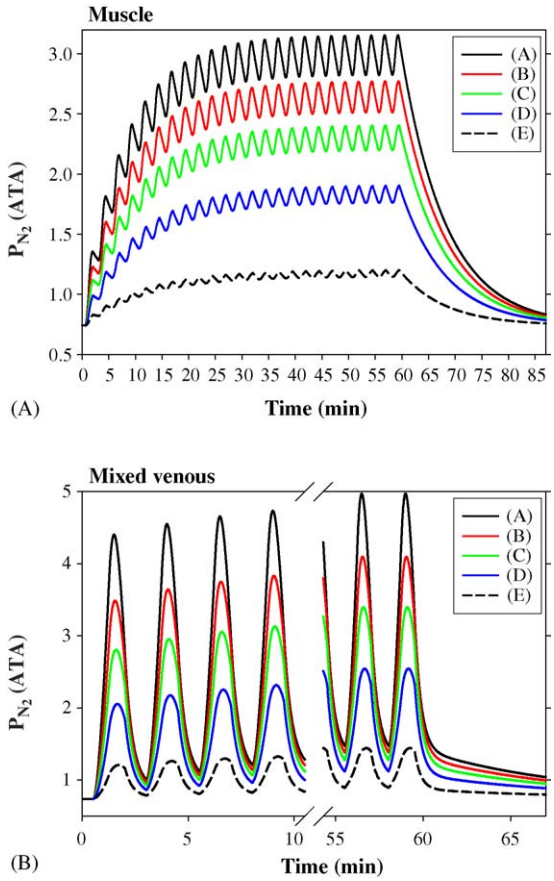

Fig. 4. Estimated (A) muscle and (B) mixed venous P_{N_2} against time in a series of 24 dives to 100 m with varying levels of pulmonary shunt (0–90%). Letters represent dive series (Table 1).

and 18 min after returning to the surface from the last dive of the bout (Ridgway and Howard, 1979).

Fig. 4 shows estimated muscle (Fig. 4A) and mixed venous P_{N_2} (Fig. 4B) against time during a dive bout with varying levels of pulmonary shunt. The pulmonary shunt was set at 0% while at the surface and then instantaneously changed as soon as the animal dove. Letters represent dive series (Table 1). Except for changes in shunt, all other variables were equivalent to dive series A (Table 1). Increased shunt fraction during diving decreased muscle and mixed venous P_{N_2} when the animal returned to the surface at the end of the dive series (Fig. 4, Table 1). With a 30% shunt, muscle and mixed venous P_{N_2} decreased by 12 and 9%, respectively. At 90% shunt P_{N_2} decreased by 62% for muscle and 64% for mixed venous, showing that P_{N_2} decreased exponentially with increasing shunt fraction.

The effect of changes in descent or ascent rate on muscle (Fig. 5A) and mixed venous P_{N_2} (Fig. 5B) are shown in Fig. 5 against time after surfacing (time 0). Letters represent dive series (Table 1). For dive series P, the ascent rate was 2.2 m·s^{-1} until 30 m below the surface followed by 1.0 m·s^{-1} until 5 m below the surface and finally at 0.5 m·s^{-1} until reaching the surface. In dive series Q, the animal experienced a dive response and a pre-surface reversal of the bradycardia at 30 m depth. Except for changes in ascent and descent rates, all other variables were equivalent to dive series A (Table 1). Increasing ascent or descent rate increased P_{N_2} and there was no effect of reversing the rate of ascent or descent on muscle P_{N_2} at the end of the dive bout (Fig. 5A, series G versus I or H versus J in Table 1). For the mixed venous compartment (Fig. 5B), surfacing P_{N_2} was higher during a rapid ascent compared with a rapid descent (Table 1). Reduction in ascent rate decreased muscle P_{N_2} by 7% and mixed venous P_{N_2} by 32% (series A versus P). This decrease occurred despite a 22% increase in DT (90 to 110 s). An additional reduction by 33% for muscle P_{N_2} and 19% for mixed venous P_{N_2} was achieved for an animal with a dive response and a pre-surface reversal of the diving bradycardia (series P versus Q).

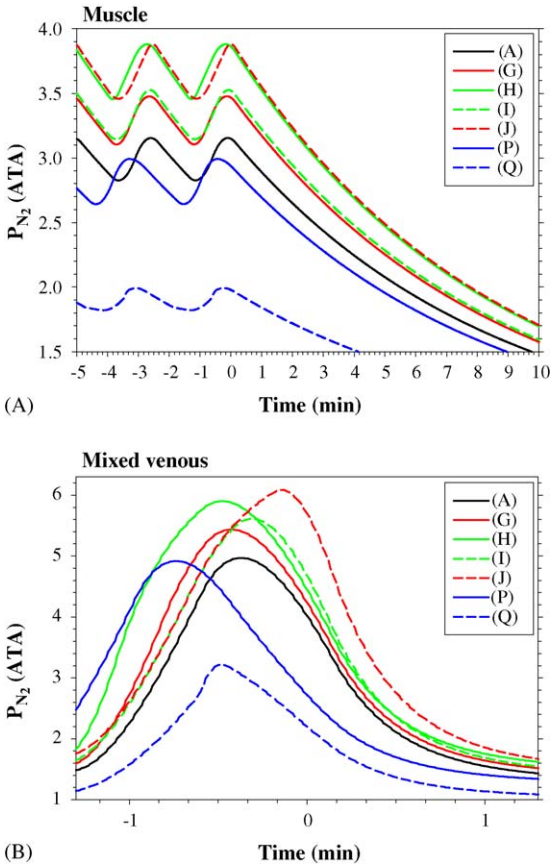

Fig. 5. Estimated (A) muscle and (B) mixed venous P_{N_2} just before and after surfacing (time 0) from the last dive in a series of 24 dives to 100 m with varying ascent and descent rates. Letters represent dive series summarized in Table 1. Except for changes in ascent rates, all other variables were the same as in Fig. 3.

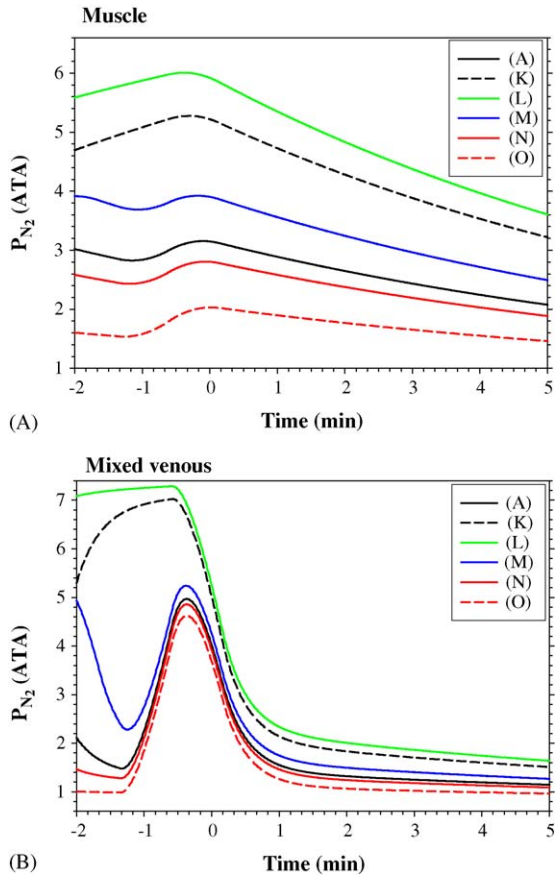

Fig. 6. Estimated (A) muscle and (B) mixed venous P_{N_2} just before and after surfacing (time 0) from the last dive in a series of 24 dives to 100 m with varying dive time (90–240 s) or surface interval (20–240 s). Letters represent dive series (Table 1). Except for changes in dive time and surface interval, all other variables were the same as in Fig. 3.

The effect of changes in DT (90–240 s) or SI (20–240 s) on muscle (Fig. 6A) and mixed venous P_{N_2} (Fig. 6B) after surfacing (time = 0) is summarized in Fig. 6. Letters represent dive series (Table 1). Except for changes in DT and SI, all other variables were the same as series A (Table 1). Changes in DT, SI or their ratio affected P_{N_2} at the end of the dive bout. In the slowly saturating muscle compartment, an increase in DT/SI ratio increased P_{N_2} (Fig. 6A, Table 1). This increase was dependent on DT and a dive with a shorter DT but with a higher DT/SI ratio resulted in lower P_{N_2}, i.e. dive series L versus M (Table 1). For the fast saturating mixed venous compartment, a 100% (series K versus A) and 167% (series L versus A) increase in DT increased mixed venous P_{N_2} by 25 and 31%, respectively (Fig. 6B). Changes in SI, on the other hand, only had a minimal effect on mixed venous P_{N_2}. An increase in SI from 20 (series M) to 240 s (series O), with a constant DT, decreased mixed venous P_{N_2} only by 13%.

4. Discussion

It was proposed by Scholander that marine mammals have lungs that collapse during breath-hold dives (Scholander, 1940). This hypothesis has been the main mechanism used to explain how breath-hold diving

animals are able to reduce blood and tissue P_{N_2} during repeated breath-hold dives, thereby preventing the bends. Studies measuring muscle (Ridgway and Howard, 1979) and arterial and venous (Kooyman et al., 1972; Falke et al., 1985) P_{N_2} values during breath-hold diving have been used as indirect evidence for lung collapse in seals and bottlenose dolphins. These studies have employed ingenious approaches to measure P_{N_2} values in various compartments. However, none of these studies have gone beyond lung collapse to account for differences in observed and expected P_{N_2} values. We modelled the role of various physiological (cardiovascular adjustment, blood flow distribution and pulmonary shunt) and behavioral (changes in dive/surface interval and ascent/descent rate) changes in inert gas dynamics to determine if any of these changes could provide alternative explanations.

4.1. Model characteristics

The current model is an oversimplification as it assumes that lung P_{N_2} remains a constant fraction of total lung pressure. However, the current model is a significant improvement from previous ones (Ridgway and Howard, 1979; Kooyman et al., 1999; Houser et al., 2001) as it accounts for changes in $\dot{Q}_{tot}$, $\dot{Q}_{tiss}$, partial pulmonary shunt and for a finite supply of N_2 during breath-hold dives. This allows direct estimation of the effect of cardiovascular adjustments or changes in inspiratory lung volume or pulmonary shunt on P_{N_2} during a diving bout. Furthermore, the model allows evaluation of changes in tissue and blood P_{N_2} kinetics with changes in M_b.

It is well-known that M_b correlates with resting metabolic rate (RMR) and $\dot{Q}_{tot}$ between species (e.g. Kleiber, 1932; Schmidt-Nielsen, 1984). Therefore, our model scaled $\dot{Q}_{tot}$ directly to M_b using an allometric mass-exponent of 0.75 assuming that $\dot{Q}_{tot}$ was directly related to metabolic rate (Schmidt-Nielsen, 1984). Less accepted is the correlation between DCS risk and M_b or DCS risk and heart rate, both within and between animal species (Flynn and Lambertsen, 1971; Berghage et al., 1979; Lillo, 1988; Lillo et al., 2002). Data from the literature show an allometric relationship between susceptibility to DCS and M_b, as well as between DCS and heart rate. The allometric mass exponents are 0.79 for M_b and 0.74 for heart rate, in seven species of animals, ranging from 22 g to 78 kg (Berghage et al., 1979). Thus, the assumption that DCS risk or P_{N_2} correlates with metabolic rate or $\dot{Q}_{tot}$ is justified and implies that larger animals are more susceptible to DCS after exposure to similar P_{N_2}'s.

The model showed that uptake and removal of N_2 was altered by changes in $\dot{Q}_{tot}$ and tissue perfusion. Whole animal $\tau_{1/2}$ was significantly altered depending on blood flow distribution. In particular, increased blood flow to tissues with larger N_2 capacitance, such as fat and muscle, without changes in $\dot{Q}_{tot}$ increased time to saturation. Thus, perfusion of subcutaneous fat may buffer against development of elevated blood P_{N_2}. This agrees with theoretical assumptions of inert gas kinetics in land animals (Kety, 1951; Mapleson, 1964).

4.2. Validation of the model

In the study by Ridgway and Howard (1979), muscle N_2 uptake and removal rates were assumed to be symmetrical with a muscle $\tau_{1/2}$ of 5.9 min. The observed muscle P_{N_2} values were lower than expected and it was concluded that lung collapse at ~70 m explained this deviation. The plausibility of this conclusion was confirmed by our model (Fig. 3) as well as by a previous study (Houser et al., 2001). However, our model analysis suggests that diving cardiovascular adjustments provide an equally plausible explanation. Breath-hold diving is associated with cardiovascular changes (dive response) and the consequences of these changes have never been estimated or even considered to affect changes in P_{N_2}. $\dot{Q}_{tot}$ probably declines during diving, especially in bottlenose dolphins in which heart rate fell from 101 beats·min^{-1} at the surface to between 44 and 51 beats·min^{-1} during dives (Noren et al., 2004). The dive response also leads to re-distribution of blood flow towards hypoxia sensitive tissues, e.g. brain and heart, and away from tissues like muscle and fat (Zapol et al., 1979). In the Weddell seal, $\dot{Q}_{muscle}$ decreased to ~6% of the pre-dive value during forced diving (Zapol et al., 1979). Therefore, changes in $\dot{Q}_{tot}$ and/or redistribution of blood flow during diving and while at the surface have a direct effect on $\tau_{1/2}$ and the assumption of a single time constant to analyze muscle P_{N_2} is not realistic (Ridgway and Howard, 1979). Certainly, the present study has shown that the deviation between expected and observed muscle P_{N_2} values is well explained by asymmetrical tissue $\tau_{1/2}$ values during diving and while at the surface (Fig. 3) suggesting that lung collapse need

not necessarily occur at depths as shallow as 70 m to yield lower than expected tissue P_{N_2}'s.

In any event, a finite supply of lung N_2 is an alternative explanation to physical alveolar collapse for lower than expected venous and arterial P_{N_2} values in seals (Kooyman et al., 1972; Falke et al., 1985). Lung collapse has previously been modelled as a gradual alveolar collapse where the compliant alveolar gas space being compressed and pushed into the non-compliant upper airways preventing further gas exchange. From these studies, the depth at which alveolar collapse occurs has been estimated to be between 30 and 160 m (Scholander, 1940; Stephenson, 2005). Others have assumed that lung collapse is instantaneous and estimated collapse depth to be between 30 and 70 m based measurements of estimates of muscle or tissue P_{N_2} (Kooyman et al., 1972; Ridgway and Howard, 1979; Falke et al., 1985). During breath-hold diving there is a finite supply of N_2 available in the lung. Still, the calculated lung collapse depths assume an infinite supply of N_2 and no alternative mechanism has been considered to explain the evidence for discontinued gas exchange. Our model suggested that in a large cetacean, with a $M_b = 1000$ kg, diving to 130 or 230 m (14 and 24 ATA), with a descent rate of 1 m·s^{-1}, lung N_2 depletes at a depth of about 100 m (∼100 s). In a smaller mammal (100 kg), depletion of lung N_2 occurs during deeper dives (14 and 24 ATA) between 345 and 580 s, while >4% of the initial number of molecules of N_2 remain for >60 min during shallow dives (4 ATA). Considering that some phocid seals are known to dive on expiration (Weddell and elephant seal, Kooyman et al., 1972), with a diving lung volume well below vital capacity (27 ml·kg^{-1}, Kooyman and Ponganis, 1998), depletion of lung N_2 alone could explain why arterial P_{N_2} values do not exceed ∼3 ATA (Kooyman et al., 1972; Falke et al., 1985). For example, in a 100 kg elephant seal with a diving lung volume of 2.7 l and descending at 1 m·s^{-1}, lung N_2 would be depleted within 80 s.

We modelled pulmonary shunt as a partial fraction of $\dot{Q}_{tot}$ during diving from 0 to 90% during dive series A for a slowly (Muscle, Fig. 4B, Table 1) and a rapidly saturating (mixed venous, Fig. 4A) compartment. A partial shunt decreased mixed venous P_{N_2} at the end of the dive bout in an exponential manner. With no shunting or during periods of nominal levels of pulmonary shunt (<30%), mixed venous P_{N_2} was governed by rapid changes in the fast responding central circulatory compartment (Fig. 4B). At a shunt fraction of 70%, mixed venous P_{N_2} decreased by 39% at the end of the dive bout compared with no shunt. Consequently, a partial pulmonary shunt has a substantial effect on inert gas uptake.

4.3. Effect of dive behavior

A doubling (series A versus K, Table 1) or tripling (series A versus L) of DT considerably increased muscle (66 and 88%, Fig. 6A) and mixed venous P_{N_2} (25 and 31%, Fig. 6B). A 66% reduction in SI increased muscle P_{N_2} by 24% (series A versus M, Table 1), but had minimal effect on the rapidly equilibrating mixed venous compartment. A tripling of SI, on the other hand, was not effective in reducing mixed venous P_{N_2} but reduced muscle P_{N_2} by 36% (series A versus O, Table 1). Consequently, P_{N_2} upon surfacing after a dive bout in a slow equilibrating tissue is dependent on both DT and SI while, in a rapidly equilibrating tissue, P_{N_2} upon surfacing depends mostly on DT. Therefore, prediction of P_{N_2} at the end of a dive bout in the slow responding muscle compartment requires knowledge of DT or SI and the ratio between DT and SI.

Increased ascent or descent rate increased P_{N_2} at the end of the dive bout (Fig. 5, Table 1). In the muscle compartment, there was minimal difference in P_{N_2} with an increase in either ascent or descent rate (Fig. 5A, Series G versus I or H versus J). For the mixed venous compartment, on the other hand, increased ascent rate increased P_{N_2} more at the end of the dive bout compared with increased descent rate (Fig. 5B). A reduction in ascent rate while approaching the surface has been observed in beluga (*Delphinapterus leucas*) and beaked whales (*Hyperoodon ampullatus*) and also in macaroni (*Eudyptes chrysolophus*) and king penguins (*Aptenodytes patagonicus*) and it has been suggested that this reduction may be an adaptation to reduce N_2 supersaturation before reaching the surface (Martin and Smith, 1992; Hooker and Baird, 1999; Sato et al., 2002, 2004). Model simulations agreed with this suggestion showing that a reduced ascent rate when approaching the surface is effective to returning N_2 to the lung before surfacing. Consequently, blood and tissue P_{N_2} supersaturation is reduced and incidence of bends is minimized.

In addition, simulations suggested a pre-surface increase in heart rate, along with a reduction in ascent rate, enhances safe transfer of N_2 from blood and

tissues back to the lung (series A versus Q), i.e. no bubble formation "en route". Therefore, the anticipatory pre-surface increase in heart rate and the higher than resting SI heart rate, and presumably increased $\dot{Q}_{tot}$, seen in diving mammals (Andrews et al., 2000) and birds (Froget et al., 2004) could be a vital adaptation to minimize P_{N_2} during diving. Increased $\dot{Q}_{tot}$ while at the surface enhances gas removal and, consequently, makes tissue levels of P_{N_2} less affected by changes in SI. Thus, our model implies that a combination of physiological and behavioural mechanisms explains how breath-hold diving animals avoid elevated levels of N_2. This could be particularly important as animal studies have shown that small changes in the inert gas load can lead to significant changes in the risk of DCS. An estimated 5% increase in the inert gas burden causes a 50% increase in observed DCS during hyperbaric experiments in pigs and rats (Kayar et al., 1998; Fahlman et al., 2001).

In summary, lung collapse has been used as an explanation for the lower than expected muscle and blood P_{N_2} values in seals and dolphins. Even though our model does not reject the possibility of lung collapse, it provides alternative explanations, such as cardiovascular adjustments or depletion of available N_2 in the lung, for a discrepancy between observed and expected P_{N_2}. Hence, re-evaluation of the depth at which lung collapse occurs and its role in DCS avoidance seems indicated. The allometric relationship between M_b and $\dot{Q}_{tot}$ enables extrapolation of venous and tissue $\tau_{1/2}$'s over several orders of magnitude. Using the estimated N_2 uptake $\tau_{1/2}$'s for a 100 kg mammal, equivalent values for a 10 kg animal would be 0.16, 41.1, 5.8 and 4.0 min for central circulation, fat, muscle and brain, respectively. For a 100,000 kg mammal, the same values would be 1.6, 398, 56.4 and 38.9 min. Since M_b correlates with dive depth and dive duration, our model is a useful tool to generate hypotheses about physiological adjustments that occur during breath-hold diving in a range of mammals. As such, it can be used to determine if the inert gas burden possibly constrains DI, SI or dive depth. Furthermore, it also yields insight into how animals with non-collapsible lungs, i.e. penguins, can modify dive behaviour to avoid elevated tissue and blood P_{N_2} during repetitive deep dives. For example, the model concurs with the suggestion that diving behavior may be an important component for reducing tissue and blood N_2 levels. A major question remains which is how can deep divers avoid the bends in the face of tissue and blood P_{N_2} that are certainly well above those that can be tolerated by their land-based relatives on rapid decompression.

Acknowledgements

This paper is dedicated to Drs. Herman Rahn and Claes Lundgren, pioneers in pulmonary and diving research, great colleague and friends. We would like to thank Dr. S. Ridgway for providing us with the body masses of the dolphins used in his study. We are grateful to Susan Kayar for her comments on the manuscript and to Peter Frappell for thought provoking discussions. Research support came from a NSERC Discovery grant to DRJ.

References

Andrews, R.D., Costa, D.P., Le Boeuf, B.J., Jones, D.R., 2000. Breathing frequencies of northern elephant seals at sea and on land revealed by heart rate spectral analysis. Respir. Physiol. 123, 71–85.

Andrews, R.D., Jones, D.R., Williams, J.D., Thorson, P.H., Oliver, G.W., Costa, D.P., Le Boeuf, B.J., 1997. Heart rates of northern elephant seals diving at sea and resting on the beach. J. Exp. Biol. 200, 2083–2095.

Berghage, T.E., David, T.D., Dyson, C.V., 1979. Species differences in decompression. Undersea Biomed. Res. 6, 1–13.

Davis, R.W., Kanatous, S.B., 1999. Convective oxygen transport and tissue oxygen consumption in Weddell seals during aerobic dives. J. Exp. Biol. 202, 1091–1113.

Dromsky, D.M., Toner, C.B., Survanshi, S., Fahlman, A., Parker, E., Weathersby, P., 2000. Natural history of severe decompression sickness after rapid ascent from air saturation in a porcine model. J. Appl. Physiol. 89, 791–798.

Eckenhoff, R.G., Olstad, C.S., Carrod, G., 1990. Human dose-response relationship for decompression and endogenous bubble formation. J. Appl. Physiol. 69, 914–918.

Fahlman, A., Kayar, S.R., 2003. Probabilistic modelling for estimating gas kinetics and decompression sickness risk in pigs during H2 biochemical decompression. Bull. Math. Biol. 65, 747–766.

Fahlman, A., Tikuisis, P., Himm, J.F., Weathersby, P.K., Kayar, S.R., 2001. On the likelihood of decompression sickness during H_2 biochemical decompression in pigs. J. Appl. Physiol. 91, 2720–2729.

Falke, K.J., Hill, R.D., Qvist, J., Schneider, R.C., Guppy, M., Liggins, G.C., Hochachka, P.W., Elliott, R.E., Zapol, W.M., 1985. Seal lungs collapse during free diving: evidence from arterial nitrogen tensions. Science 229, 556–558.

Farhi, L.E., 1967. Elimination of inert gas by the lung. Respir. Physiol. 3, 1–11.

Flynn, E.T.J., Lambertsen, C.J., 1971. Calibration of inert gas exchange in the mouse. In: Lambertsen, C.J. (Ed.), Underwater Physiology. Academic Press, New York, pp. 179–191.

Froget, G., Butler, P.J., Woakes, A.J., Fahlman, A., Kuntz, G., Le Maho, Y., Handrich, Y., 2004. Heart rate and energetics of free ranging king penguins (*Aptenodytes patagonicus*). J. Exp. Biol. 207, 3917–3926.

Hills, B.A., 1977. Decompression Sickness. John Wiley & Sons, New York.

Hlastala, M.P., van Liew, H.D., 1975. Absorption of in vivo inert gas bubbles. Respir. Physiol. 24, 147–158.

Hooker, S.K., Baird, R.W., 1999. Deep-diving behaviour of the northern bottlenose whale, *Hyperoodon ampullatus* (Cetacea: Ziphiidae). Proc. R. Soc. Lond. B Biol. Sci. 266, 671–676.

Houser, D.S., Howard, R., Ridgway, S., 2001. Can diving-induced tissue nitrogen supersaturation increase the chance of acoustically driven bubble growth in marine mammals? J. Theor. Biol. 213, 183–195.

Kayar, S.R., Aukhert, E.O., Axley, M.J., Homer, L.D., Harabin, A.L., 1997. Lower decompression sickness risk in rats by intravenous injection of foreign protein. Undersea Hyperb. Med. 24, 329–335.

Kayar, S.R., Miller, T.L., Wolin, M.J., Aukhert, E.O., Axley, M.J., Kiesow, L.A., 1998. Decompression sickness risk in rats by microbial removal of dissolved gas. Am. J. Physiol. 275, R677–R682.

Kety, S.S., 1951. The theory and applications of the exchange of inert gas at the lungs and tissues. Pharmacol. Rev. 3, 1–41.

Kleiber, M., 1932. Body size and metabolism. Hilgarida 6, 315–353.

Kooyman, G.L., Ponganis, P.J., 1998. The physiological basis of diving to depth: birds and mammals. Annu. Rev. Physiol. 60, 19–32.

Kooyman, G.L., Ponganis, P.J., Howard, R.S., 1999. Diving animals. In: Lundgren, C.E.G., Miller, J.N. (Eds.), The Lung at Depth. Marcel Dekker, Inc., New York, pp. 587–620.

Kooyman, G.L., Schroeder, J.P., Denison, D.M., Hammond, D.D., Wright, J.J., Bergman, W.P., 1972. Blood nitrogen tensions of seals during simulated deep dives. Am. J. Physiol. 223, 1016–1020.

Lillo, R.S., 1988. Effect of N2-He-O2 on decompression outcome in rats after variable time at depth dives. J. Appl. Physiol. 64, 2042–2052.

Lillo, R.S., Flynn, E.T., Homer, L.D., 1985. Decompression outcome following saturation dives with multiple inert gases in rats. J. Appl. Physiol. 59, 1503–1514.

Lillo, R.S., Himm, J.F., Weathersby, P.K., Temple, D.J., Gault, K.A., Dromsky, D.M., 2002. Using animal data to improve prediction of human decompression risk following air saturation dives. J. Appl. Physiol. 93, 216–226.

Lillo, R.S., Parker, E.C., Porter, W.R., 1997. Decompression comparison of helium and hydrogen in rats. J. Appl. Physiol. 82, 892–901.

Mapleson, W.W., 1964. Inert gas-exchange theory using an electric analogue. J. Appl. Physiol. 19, 1193–1199.

Martin, A.R., Smith, T.G., 1992. Deep diving in wild free-ranging beluga whales (*Delphinapterus leucas*). Can. J. Fish Aquat. Sci. 49, 462–466.

Noren, S.R., Cuccurullo, V., Williams, T.M., 2004. The development of diving bradycardia in bottlenose dolphins (*Tursiops truncatus*). J. Comp. Physiol. [B] 174, 139–147.

Olszowka, A.J., Rahn, H., 1987. Gas store changes during repetitive breath-hold diving. In: Shiraki, K.S., Yousef, M.K. (Eds.), Man in Stressful Environment-Diving, Hyperbaric and Hypobaric Physiology. Charles C Thomas Publisher, Springfield, pp. 417–428.

Paulev, P., 1965. Decompression sickness following repeated breath-hold dives. J. Appl. Physiol. 20, 1028–1031.

Paulev, P.E., 1967. Nitrogen tissue tensions following repeated breath-hold dives. J. Appl. Physiol. 22, 714–718.

Ridgway, S.H., Howard, R., 1979. Dolphin lung collapse and intramuscular circulation during free diving: evidence from nitrogen washout. Science 206, 1182–1183.

Sato, K., Charrassin, J.B., Bost, C., Naito, Y., 2004. Why do macaronu penguins choose shallow body angles that result in longer descent and ascent durations? J. Exp. Biol. 207, 4057–4065.

Sato, K., Naito, Y., Kato, A., Niizuma, Y., Watanuki, Y., Charrassin, J.B., Bost, C.A., Handrich, Y., Le Maho, Y., 2002. Buoyancy and maximal diving depth in penguins: do they control inhaling air volume? J. Exp. Biol. 205, 1189–1197.

Schmidt-Nielsen, K., 1984. Scaling: Why is Animal Size So Important? Cambridge University Press, Cambridge.

Scholander, P.F., 1940. Experimental Investigations on the Respiratory Function In Diving Mammals and Birds. Hvalrådets skrifter, 22.

Stephenson, R., 2005. Physiological control of diving behaviour in the Weddell seal Leptonychotes weddelli: a model based on cardiorespiratory control theory. J. Exp. Biol. 208, 1971–1991.

Ward, C.A., McCullough, D., Fraser, W.D., 1987. Relation between complement activation and susceptibility to decompression sickness. J. Appl. Physiol. 62, 1160–1166.

Weathersby, P.K., Homer, L.D., 1980. Solubility of inert gases in biological fluids and tissues: a review. Undersea Biomed. Res. 7, 277–296.

Weathersby, P.K., Homer, L.D., Flynn, E.T., 1984. On the likelihood of decompression sickness. J. Appl. Physiol. 57, 815–825.

Weathersby, P.K., Survanshi, S.S., Homer, L.D., Parker, E., Thalmann, E.D., 1992. Predicting the time of occurrence of decompression sickness. J. Appl. Physiol. 72, 1541–1548.

Zapol, W.M., Hill, R.D., Qvist, J., Falke, K., Schneider, R.C., Liggins, G.C., Hochachka, P.W., 1989. Arterial gas tensions and hemoglobin concentrations of the freely diving Weddell seal. Undersea Biomed. Res. 16, 363–373.

Zapol, W.M., Liggins, G.C., Schneider, R.C., Qvist, J., Snider, M.T., Creasy, R.K., Hochachka, P.W., 1979. Regional blood flow during simulated diving in the conscious Weddell seal. J. Appl. Physiol. 47, 968–973.